RRPC91080489 (10.P)

行政院國家科學委員會補助專題研究計畫成果報告

細胞支架於肝臟細胞色素 P450 酵素代謝麻醉藥物 Propofol 中扮演的角色(1/3)

計畫類別：☒個別型計畫　□整合型計畫
計畫編號：NSC91-2314-B-038-029-
執行期間：91 年 08 月 01 日至 92 年 07 月 31 日

計畫主持人：陳大樑
共同主持人：

本成果報告包括以下應繳交之附件：

□赴國外出差或研習心得報告一份
□赴大陸地區出差或研習心得報告一份
□出席國際學術會議心得報告及發表之論文各一份
□國際合作研究計畫國外研究報告書一份

執行單位：台北醫學大學醫學系麻醉學科

中　華　民　國　92　年　04　月　29　日

行政院國家科學委員會專題研究計畫成果報告

細胞支架於肝臟細胞色素 P450 酵素代謝麻醉藥物 Propofol 中扮演的角色(1/3)

THE ROLE OF CYTOSKELETON IN HEPATIC DRUG METABOLISM OF PROPOFOL BY CYTOCHROME P450 ENZYMES

計畫編號：NSC 91-2314-B-038-029-
執行期限：91 年 08 月 01 日至 92 年 07 月 31 日
主持人：陳大樑　台北醫學大學醫學系麻醉學科
計畫參與人員：陳瑞明、林怡伶、王嫻琪 台北醫學大學醫學系麻醉學科

Introduction

麻醉藥物的代謝，主要是靠肝臟細胞色素 P450 單氧酵素系統 (Cytochrome P450 monooxygenase system) 的多種同型酵素 (Isozymes) 對於受質 (Substrates) 之特異性 (Specificity) 結合關係，進行各種化學分解反應，以達到活化 (Activation) 或去活化 (Inactivation) 的酵素功能[1]。Propofol (此為學名；結構名為 2,6-雙異丙烷酚；商品名為 Diprivan) 為一油溶性製劑之靜脈麻醉劑，目前廣泛被用於麻醉誘導，以及持續性維持麻醉之用 (Glen 等, 1980 and 1984)[2,3]。其藥物動力學有諸多優點，包括高脂溶性，廣泛再分佈於各組織，及其可預期之作用和藥效時間，使得它普遍地被使用於各種手術，並可配合不同長短時間的需求 (Cockshott 等, 1985 and 1987)[4,5]。Propofol 主要的代謝產物，是形成去活化之葡萄糖苷酸 (glucuronide) 結合物，及其相對之對苯三醇化物 (quinol) (2,6-雙異丙烷酚-1.4-對苯三醇)，而所依賴之代謝酵素，即是細胞色素 P450 單氧酵素系統 (Simons 等, 1988)[6]。如有其他需要靠此酵素群代謝之藥物或外來物，同時給予病患時，則理論上無可避免地將會與 Propofol 產生藥物動力學上之干擾。

以上這些論著，研究探討的領域多半是在酵素學 (Enzymology) 方面，過去數年來，本研究室持續對於細胞色素 P450 的代謝功能及麻醉藥物 Propofol 的交互作用，進行動物及人類肝、腎細胞之研究，使用酵素學及生化的方法探討藥理學的領域[7-14]。細胞色素 P450 酵素群對於外來物及麻醉藥物的代謝，主要是在內質網 (Endoplasmic reticulum, ER) 進行，然而外來物與藥物是藉由何種路徑及方式，由細胞膜傳送至內質網酵素進行代謝，以及與其他胞器，如高基氏體 (Golgi apparatus) 甚至與細胞核膜之間，細胞支架 (Cytoskeleton) 的運送和互動角色，尚不清楚，機轉方面也只有間接的推測，而缺乏直接證據。近年來本人嘗試將細胞生物學 (Cellular biology) 的研究方法，以共軛焦顯微鏡 (Confocal laser scanning microscope) 為研究工具，運用於麻醉學及藥物作用方面之研究；第一個方向是以細胞內鈣離子的移動與粒線體功能為主軸，觀察 Propofol 對細胞功能抑制的可能機轉[15,16]。

首先以目前認為最影響細胞功能的介質-鈣離子為研究主題，使用細胞株 Gm 7372a (牛主動脈內皮細胞株)，以 Fluo-3

螢光染色後，在共軛焦顯微下觀察其基礎狀態；而後用 bradykinin 激發細胞內鈣的釋放，形成細胞中大量的熱亮點 (hot spots)，謂之激發狀態；但如將內皮細胞先與濃度 10^{-5} M 的 propofol 共存後，激發狀態的內鈣釋送情形，則會大幅受到抑制。

再來則是探討 propofol 使內鈣釋放減少的機制，包括對細胞內胞器膜通透性的抑制，如以 Ionophore (Ionomycin) 打開胞膜通道，以共軛焦顯微鏡可見內鈣大量的釋出，但如先以濃度 10^{-5} M 的 propofol 處理內皮細胞，則可見此釋放受到抑制，意謂 Propofol 對於胞器膜之通透，亦可造成一定程度的抑制。

進一步就 propofol 對於細胞內胞器的功能，如對粒線體 (mitochondria) 的影響進行探討，在共軛焦顯微鏡下，我們以 DiOC6 觀察內皮細胞粒線體膜動作電位，發現如以 10^{-5} M propofol 處理之後，明顯會干擾下降粒線體之動作電位；再以 TM Ros 染色觀察粒線體的型態，發現 10^{-5} M propofol 可以產生類似粒線體 uncoupler, 如 carbonylcyanide *p*-trifluoromethoxy phenylhydrazone (FCCP)對粒線體型態的破壞現象，顯示 propofol 對於粒線體的動作電位與型態，均會造成一定程度的干擾與抑制 (見下圖)。

第二個方向則是嘗試運用共軛焦顯微鏡技術，探討活細胞在代謝過程中，細胞支架 (Cytoskeleton) 於細胞內運送藥物（如：Propofol）時扮演的角色與其機制，以及對細胞色素 P450 代謝外來麻醉藥物 Propofol 的影響為何。細胞支架是活體細胞負責細胞間張力或細胞內傳送物質的主要通道，其動態的再造 (Dynamic remodeling) 可形成細胞內機械力的平衡，導致細胞間之傳導及內在結構的重建 (Reorganization) [17, 18]。有關細胞色素 P450 酵素群在細胞內 (如肝細胞) 所扮演的代謝角色，學術界已有相當深度的認識與探討，然而由細胞膜運送受質到內質網以及細胞核膜≒內質網≒高基氏體≒ 細胞膜之間的運送機轉，進而如何影響細胞色素 P450 的功能，則是一個嶄新的研究領域。在以往無法動態性地了解活細胞有關這類方面的功能，主

要是受限於沒有適當的觀察工具，但是 1994 年 Denk 等人發展出共軛焦顯微鏡及雙光子雷射掃瞄顯微鏡 (Two-photon laser scanning microscope) 以後 [19]，開啟此新方向，逐漸有人探討細胞 P450 酵素與受質間，如何在膜與膜之間的細胞支架上運送。Robin 等人 (Gastroenterology 1995;108:1110-23) 首先探索 P450 2B 似乎是以泡狀型式 (Vesicular route) 在細胞膜間運送 [20]，接著 Anderson 等人嘗試在培養活細胞內，觀察肝細胞的動態代謝功能 (Int. J. Artificial Organ 1998;21:360-4) [21]，最近 Tzanakakis 等人更進一步探討 CYT 2B 在肝細胞內執行代謝功能時，與細胞支架可能的互動關係為何 (Cell Motility & the Cytoskeleton 2001;48:175-89) [22]。

然而在麻醉藥物與細胞色素 P450 代謝功能的方向上，目前尚未有任何研究，探索細胞支架在代謝麻醉藥物上所扮演的角色，本研究計劃嘗試以開創性的研究方法，來探討在肝細胞培養系統中，藉由特殊之培養介面 (Primaria; Becton Dickinson, Franklin Lakes, NJ, USA)，使肝細胞由於細胞內支架之作用，自我形成立體球體 (Spheroid self-assembly) [17, 18, 22]，在此模式下，再以各種藥理物質干擾細胞支架的形成，同時以其共軛焦顯微鏡活體觀察 CYT P450 酵素代謝螢光受質的代謝情形，是否受細胞支架被干擾而有所改變，再用 HPLC 以分析 Propofol 代謝後之產物，以釐清細胞色素 P450 代謝 Propofol 時，細胞支架所扮演的關鍵角色。

Materials and Methods

Hepatocyte Culture

Hepatocytes were harvested from 4-6-week-old male Sprague-Dawley rats weighing 200-250 g by a modified two-step in situ collagenase perfusion technique (Seglen, 1976) [23]. The hepatocyte viability after the harvest ranged from 90% to 95% based on trypan blue exclusion. Hepatocytes were cultivated in basal Williams' E medium (Life Technologies, Grand Island, NY)

supplemented with 50 ng/ml epidermal growth factor (Sigma Chemical Co., St. Louis, MO), 0.2×10^{-3} U/ml insulin (Lilly Research Laboratories, Indianapolis, IN), 50 ng/ml linoleic acid (Sigma), 0.1 U/ml penicillin (Life Technologies), 100 μg/L streptomycin (Life Technologies), 2 mM L-glutamate (LifeTechnologies), 0.1 μm copper ($CuSO_4 \cdot 5H_2O$), 50 pM zinc ($ZnSO_4 \cdot 7H_2O$), 3nM selenium (H_2SeO_3) and 15 mM *N*-(2-hydroxyethyl)piperazine-*N'*-2-ethanesulfonic acid (HEPES) (Life Technologies). Hepatocytes were cultured on 35-mm Falcon Primaria dishes (Becton Dickinson, Franklin Lakes, NJ) at approximately 40,000 cells/cm^2. Six to twelve hours after inoculation, the medium was withdrawn to remove unattached cells and fresh medium was added. In the experiments involving cytoskeleton-disorganizing drugs, cytochalasin D (Aldrich, Milwaukee, WI), taxol, or nocodazole (Cytoskeleton, Denver, CO) were added to a final concentration of 1-20 um at the time of medium replenishment. The drugs were kept in the cultures until the end of each experiment.

Determination of viability with confocal microscope

Hepatocytes were dually stained with fluorescein diacetate (FDA) (Sigma) and ethidium bromide (EB) (Sigma) as described previously (Nikolai et al., 1991)[24]. The intracellular esterases cleave the FDA to fluorescein only in viable cells. EB penetrates dead cells and intercalates with the nuclear DNA. Under a fluorescence microscope, the viable cells appear green whereas the nuclei of non-viable cells appear bright red. Samples were observed with an epifluorescence inverted microscope (Olympus IX 70) connected to a confocal laser scanning system (Model FV500, Olympus, Japan). The excitation wavelength was 488 nm and the emitted light was directed through a 595-nm beam splitter; light of wavelength less than 595 nm was filtered through a 530 nm band pass filter (30-nm window) to detect FDA staining. Light emitted at greater then 595 nm was filtered through a 600-nm long-pass filter to detect EB staining. The pinhole aperture was set to 50 μm. Each sample was scanned in a raster fashion to produce side-by-side 512x 512 pixel images. Hepatocyte viability was evaluated by counting the number of FDA-stained and EB-stained cells on the acquired images.

Actin Staining of Hepatocytes

The actin filaments in hepatocytes were visualized by phalloidin immuno-fluorescence staining. Cells on monolayers were stained 24 to 48 h after plating. After washing with 2 mL of phosphate-buffered saline (PBS), cells were fixed with 4% paraformaldehyde for 10 min at room temperature and then were permeabilized for 15 min in 0.2% Triton X-100 (Sigma) and 0.1% bovine serum albumin (BSA) (Sigma) in PBS at room temperature. Cells were then stained for 15 min with 0.5 μg/ml rhodamine-phalloidin (Molecular Probes, Eugene, OR) in PBS (working solution). After washing the cells with PBS, a drop of PVA-glycerol (0.2 g/ml polyvinylalcohol [Sigma] in a 1:2 mixture of glycerol [Sigma] and PBS) was added to each sample before applying coverslips. The samples were stored in the dark at 4℃ until examination. A confocal laser scanning microscope (Model FV500, Olympus, Tokyo, Japan) was utilized for sample observation. An Olympus PlanApo 60x/1.4 NA oil-immersion objective lens was used to visualize actin filaments. The excitation wavelength was set to 568 nm while a 585 nm long-pass filter was utilized to collect the emitted light. Images were acquired using the FLUOVIEW software (version 4.0, Olympus Optical Co. Ltd., Tokyo, Japan).

In the case of spheroids, samples from 4-day cultures were transferred to 15-ml centrifuge tubes. After washing twice with 10 ml PBS, the spheroids were allowed to settle by

gravity, transferred to glass Lab-Tek slides (Nunc, Naperville, IL), and fixed for 1 h in 4% paraformaldehyde in PBS. The fixed spheroids were washed in PBS for 20 min followed by permeabilization overnight at 4 ℃ using the same solution as that used for monolayer cultures. The conditions for rhodamine-phalloidin staining were the same as that for monolayer cultures except that the staining period was 1 h. The silicon gasket of Lab-Tek slides was removed and a drop of the PVA-glycerol mixture was added to each sample. Coverslips were applied on top of the samples and sealed with nail polish. The spheroid samples were observed under a two-photon excitation fluorescence microscope (Mira 900-F laser and Verdi ^{TM} V-5, Coherent Laser Group, Santa Clara, CA, USA) using a 10 objective lens and pulsed laser at 1,000nm.

In Situ Assessment of CYP450 Activity

To probe for the rat cytochrome P450 2B1/2 (CYP2B1/2) activity in hepatocyte cultures, the pentoxyresofurin-O-depentylation (PROD) reaction was employed. Non-fluorescent pentoxyresorufin is a specific substrate for rat CYP2B1/2 (Burke et al., 1994) [35]. The product of the PROD reaction is fluorescent resorufin. Detection of resorufin in cells and cell aggregates is performed using confocal laser scanning microscopy (Heinomen et al., 1996; Sidhu et al., 1993) [36, 37].

In situ detection of PROD activity was employed in this study. Briefly, culture medium was replaced with 2 ml of pre-warmed incubation buffer and incubated for 5 min in a humidified, 5% CO2, 37 ℃ incubator. The incubation buffer was Williams' E medium without phenol red supplemented with 2 mM probenicid (Sigma), an inhibitor of glucoronidation, and 25 μM dicumarol (Sigma), a specific inhibitor of DT-diaphorase. Dicumarol inhibits further metabolism of resorufin (Cretton and Sommadossi, 1991) [38] to non-fluorescent metabolites. The aqueous stock solutions of 0.2 M probenicid and 10 mM dicumarol were prepared in 0.5 N NaOH. The pH of the incubation buffer was adjusted to 7.2 with 1.0 M HEPES. The PROD reaction was initiated by the addition of medium containing 20 μM pentoxyresorufin was at 1 mM in DMSO. Confocal microscopy was employed to determine the PROD activity using a 10x/0.45 NA objective lens. The excitation wavelength was 514 nm. A 570-nm long-pass filter was used to detect the emitted fluorescent intensity with wavelengths longer than 570 nm. The pinhole aperture was set to 100 μm .The voltage of the photomultiplier tubes was held constant throughout all 512 x 512 pixel micrographs that were scanned. A pseudocolor map was implemented to facilitate the visual comparison of the PROD activity of cells under different culture conditions.

Determination of Propofol Concentration and its Metabolites by High Performance Liquid Chromatography (HPLC) Analysis

The high-performance liquid chromatograph used consisted of a solvent delivery system set to deliver a solvent flow of 1.5 ml/min, an automatic sample injector and a fluorescence detector. The excitation and emission wavelengths were 276 and 310 nm, respectively, and both monochromator slit widths were 10 nm. A C_{18} reversed-phase column was used at ambient temperature.

Microsomal propofol hydroxylation activities were determined as described (Court et al., 1999)[39]. The dry residues of propofol and its metabolites from in vitro metabolism by rat liver microsomes was redissolved in HPLC mobile phase (200 μl) and an aliquot (100 μl) of the solute was submitted to HPLC analysis. The mobile phase consisted of 50% acetonitrite, 40% water and 10% methanol with a flow rate 2ml/mim. A standard curve was generated by assay of samples containing varying amounts of a fixed amount of internal standard. Metabolite concentrations were then calculated by linear regression of calibration curve data using the measured metabolite-

internal standard peak height ratios. Enzyme activity was calculated by dividing the amount of product formed by incubation time and microsomal protein content, and expressed as nmol/min/mg. Incubation time (10 min) and microsomal protein concentration (100 μg/ml) were minimized to ensure linearity of product formation with respect to these variables.

Statistical Analysis

Cells from at least 4 separate incubation plates with n = 10 were examined. The image analysis of the results allowed the fluorescence per cell (fluorescent intensity, in arbitrary units) to be quantified. The activities of cytochrome P450 2B1/2 (PROD) and HPLC analyses of metabolites of propofol before and after the addition of compounds interrupting cytoskeleton of hepatocyte were analyzed with repeated measurements of ANOVA. Results are means ± SEM. $P < 0.05$ was considered significantly different when comparing with the corresponding control.

Results

Administration of hepG2 cells with 1, 25, 75 and 100 μM propofol for 1, 6 and 24 hours did not affect cell viability (Table 1). However, when the concentration of propofol reach 300 and 1000 μM, the viability of HepG2 cell significantly decreased.

The density of F-actin in HepG2 cells exposed to 50 μM propofol for 1 hour was apparently reduced (Fig. 1). The suppressive effect was lasted to 6 hours. Quantification of the F-actin intensity in control and propofol-treated HepG2 cells was carried out and the results were shown in Fig. 2.

In untreated HepG2 cells, the PROD activity was detectable (Fig. 3). Following phenobarbital treatment, the PROD activity was significantly augmented. RT-PCR analysis of CYP2B6 revealed that exposure to phenobarbital for 24 and 48 hours induced CYP2B6 mRNA (Fig. 4).

Confocal analysis of pentoxyresorufin metabolism by CYP2B6 in HepG2 cells revealed that the levels of 7-hydroxyresorufin, a fluorescent metabolite, in phenobarbital-treated HepG2 cells were significantly more than control cells (Figs. 5 and 6).

References

1. Guengerich FP, Shimada T: Oxidation of toxic and carcinogenic chemicals by human cytochrome P450 enzymes. Chem Res Toxicol 1991; 4: 391-407.
2. Glen JB: The animal pharmacology of ICI 35,868: A new i.v. anaesthetic agent. Br J Anaesth 1980; 52: 230P.
3. Glen JB, Hunter SC: Pharmacology of an emulsion formulation of ICI 35,868. Br J Anaesth 1984; 56: 617-626.
4. Cockshott ID: Propofol (Diprivan) pharmacokinetics and metabolism – an overview. Postgrad Med J 1985; 61: 45-50.
5. Cockshott ID, Briggs LP, Douglas EJ, White M: Pharmacokinetics of propofol in female patients. Studies using single bolus injections. Br J Anaesth 1987; 59: 1103-1110.
6. Simons PJ, Cockshott ID, Douglas EJ, Gordon EA, Hopkins K, Rowland M: Disposition in male volunteers of a subanaesthetic intravenous dose of an oil in water emulsion of ^{14}C-propofol. Xenobiotica 1988; 18: 429-440.
7. Chen TL, Wu CH, Chen TG, Tai YT, Chang HC, Lin CJ: Effects of propofol on functional activities of hepatic and extrahepatic conjugation enzymes systems. British Journal of Anaesthesia 2000; 84: 771-776.
8. Chen TL, Chen TG, Tai YT, Chang HC, Chen RM, Lin CJ, Ueng TH: Propofol inhibits renal cytochrome P450 activity and enflurane defluorination in vitro in hamsters. Canadian Journal of Anaesthesia 2000; 47: 680-686.
9. Chen TL, Chang HC, Chen TG, Tai YT, Chen RM: Modulation of cytochrome P-450 dependent monooxygenases in streptozotocin-induced diabetic hamster: I. Effects of propofol on defluorination and cyt. P-450 activities. Acta Anaesthesiologica Sinica 2000; 38: 15-21.
10. Chen TG, Tai YT, Chang HC, Hong CT, Chen RM, Chen TL: Modulation of cytochrome

P450-dependent monooxygenases in streptozotocin-induced diabetic hamster: II. Reverse role of insulin in P450 activity and defluorination. Acta Anaesthesiologica Sinica 2000; 38: 65-72.

11. Chen TL, Hou WY, Sun WZ, Wu GJ, Wang KC, Peng WL, Lin CJ: Metabolic characteristics and enflurane defluorination of cytochrome P450-dependent monooxygenases in human hepatocellular carcinoma. Acta Anaesthesiologica Sinica 1997; 35: 7-14.
12. Chen TL, Chen SH, Tai TY, Chao CC, Park SS, Guengerich FP, Ueng TH: Induction and suppression of renal and hepatic cytochrome P450-dependent monooxygenase by acute and chronic streptozotocin diabetes in hamsters. Archives of Toxicology 1996; 70: 202-208.
13. Chen TL, Ueng TH, Chen SH, Lee PH, Fan SZ, and Liu CC: Human cytochrome P450 monooxygenase system is suppressed by propofol. British Journal of Anaesthesia 1995; 74: 558-562.
14. Chen TL, Wang MJ, Huang CH, Liu CC, Ueng TH: Difference between in vivo and in vitro effects of propofol on defluorination and metabolic activities of hamster hepatic cytochrome P450-dependent monooxygenases. British Journal of Anaesthesia 1995; 75: 462-466.
15. Tai YT, Wu CC, Wu GJ, Chang HC, Chen TG, Chen RM, Chen TL: Study of propofol in bovine aortic endothelium: I. Inhibitory effect on bradykinin-induced intracellular calcium immobilization. Acta Anaesthesiologica Sinica 2000; 38: 181-186.
16. Chang HC, Tsai SY, Wu GJ, Lin YH, Chen RM, Chen TL: Effects of propofol on mitochondrial function and intracellular calcium shift in bovine aortic endothelial model. Acta Anaesthesiologica Sinica 2001; 39: 115-122.
17. Ingber DE, Dike L, Hansen L, Karp S, Liley H, Maniotis A, McNamee H, Mooney D, Plopper G, Sims J, Wang N: Cellular tensegrity: exploring how mechanical changes in the cytoskeleton regulate cell growth, migration, and tissue pattern during morphogenesis. Int Rev Cytol 1994; 150: 173-224.
18. Mooney DJ, Langer R, Ingber DE: Cytoskeletal filament assembly and the control of cell spreading and function by extracellular matrix. J Cell Sci 1995; 108: 2311-2320.
19. Denk W, Delaney KR, Gelperin A, Kleinfeld D, Strowbridge BW, Tank DW, Yuste R: Anatomical and functional imaging of neurons using 2-photon laser scanning microscopy. J Neuroscience Methods 1994; 54: 151-162.
20. Robin MA, Maratrat M, Loeper J, Durand-Schneider AM, Tinel M, Ballet F, Beaune P, et al.: Cytochrome P4502B follows a vesicular route to the plasma membrane in cultured rat hepatocytes. Gastroenterology 1995; 108: 1110-1123.
21. Anderson K, Wilkinson R, Grant MH: Assessment of liver function in primary cultures of hepatocytes using diethoxy (5,6) chloromethylfluorescein and confocal laser scanning microscopy. The International Journal of Artificial Organs 1998; 21: 360-364.
22. Tzanakakis ES, Hansen LK, Hu WS: The role of actin filaments and microtubules in hepatocyte spheroid self-assembly. Cell Motility and the Cytoskeleton 2001; 48: 175-189.
23. Seglen PO: Preparation of isolated rat liver cells. Methods Cell Biol.1976; 13: 29-83.
24. Nikolai TJ, Peshwa MV, Goetghebeur S, Hu WS: Improved microscopic observation of mammalian cells on microcarriers by fluorescent staining. Cytotechnology 1991; 5: 141-146.
25. Jäntti J, Kuismanen E: Effect of caffeine and reduced temperature (20℃) on the organization of the pre-Golgi and the Golgi stack membranes. J Cell Biol 1993; 120: 1321-1335.
26. Estes JE, Selden LA, Gershman LC: Mechanism of action of phalloidin on the polymerization of muscle actin. Biochemistry 1981; 20: 708-712.
27. Hamel E: Natural products which interact with tubulin in the vinca domain: maytansine, rhizoxin, phomopsin A, dolastatins 10 and 15 and halichondrin B. Pharmacol Ther 1992; 55: 31-51.
28. Mollenhauer HH, Morré DJ, Rowe LD: Alteration of intracellular traffic by monensin; mechanism, specificity and relationship to toxicity. Biochim Biophys Acta 1990; 1031: 225-246.
29. Miller SG, Carnell L, Moore HPH: Post-Golgi membrane traffic: brefeldin A inhibits export from distal Golgi compartments to the cell surface but not recycling. J Cell Biol 1992; 118: 267-283.
30. Hastie SB: Interactions of colchicine with tubulin. Pharmacol Ther 1991; 51: 377-401.
31. MacLean-Fletcher S, Pollard TD: Mechanism of action of cytochalasin B on actin. Cell 1980; 20: 329-341.
32. Manfredi JJ, Fant J, Horwitz SB: Taxol induces the formation of unusual arrays of cellular microtubules in colchicine-pretreated J774.2 cells. Eur J Cell Biol 1986; 42: 126-134.
33. Samson F, Donoso JA, Heller-Bettinger I, Watson D, Himes RH: Nocodazole action on

tubulin assembly, axonal ultra-structure and fast axoplasmic transport. J Pharmacol Exp Therapeut 1979; 208: 411-417.

34. Peshwa MV, Wu FJ, Follstad BD, Cerra FB, Hu WS: Kinetics of hepatocyte spheroid formation. Biotechnol Prog 1994; 10: 460-466.

35. Burke MD, Thompson S, Elcombe CR, Halpert J, Haaparanta T, Mayer RT: Ethoxy-, pentoxy- and benzyloxyphenoxazones and homologues: a series of substrates to distinguish between different induced cytochromes P-450. Biochem Pharmacol 1985; 34: 3337-3345.

36. Heinomen JT, Sidhu JS, Reilly MT, Farin FM, Omiecinski CJ, Eaton DL, Kavanagh TJ: Assessment of regional cytochrome P450 activities in rat liver slices using resorufin substrates and fluorescence confocal laser cytometry. Environ Health Perspect 1996; 104: 536-543.

37. Sidhu JS, Kavangh TJ, Reilly MT, Omiecinski CJ: Direct determination of functional activity of cytochrome P450 1A1 and NADPH DT-diaphorase in hepatoma cell lines using non-invasive scanning laser cytometry. J Toxicol Environ Health 1993; 40: 177-194.

38. Cretton EM, Sommadossi JP: Modulation of 3'-Azido-3'-deoxythymidine catabolism by probenecid and acetaminophen in freshly isolated rat hepatocytes. Biochem Pharmacol 1991; 42: 1475-1480.

39. Court MH, Hay-Kraus BL, Hill DW, Kind AJ, Greenblatt DJ: Propofol hydroxylation by dog liver microsomes: assay development and dog breed difference. Drug Metabolism and Disposition 1999; 27: 1293-1299.

Table 1 Effect of propofol on the viability of HepG2 cells

Conc.	Cell viability, OD_{550}		
(μM)	1h	6h	24h
0	1.05 ± 0.08	1.28 ± 0.02	0.34 ± 0.03
1	0.98 ± 0.08	1.43 ± 0.06	0.34 ± 0.02
25	0.98 ± 0.09	1.25 ± 0.03	0.33 ± 0.03
50	0.96 ± 0.08	1.25 ± 0.07	0.32 ± 0.03
75	1.00 ± 0.06	1.09 ± 0.02*	0.32 ± 0.02
100	0.86 ± 0.05	1.22 ± 0.02	0.27 ± 0.03
300	0.79 ± 0.05*	1.00 ± 0.06*	0.13 ± 0.02*
1000	0.15 ± 0.02*	0.10 ± 0.01*	0.14 ± 0.01*

HepG2 cells were treated with various concentrations of propofol for 1, 6 and 24 hours. Cell viability was assayed by the MTT assay. Each value is represented as Mean ± SEM for n = 6. *Values significantly different from the respective control, $P < 0.05$.

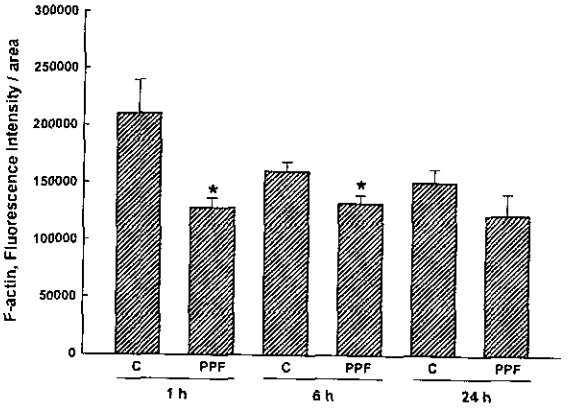

Fig. 2 Quantification of propofol-caused suppressive effects on F-actin of HepG2 cells.

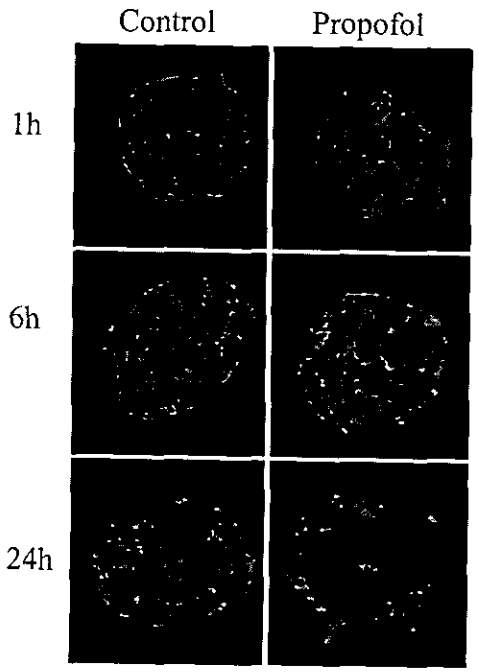

Fig. 1 Effect of propofol on F-actin of HepG2 cells.

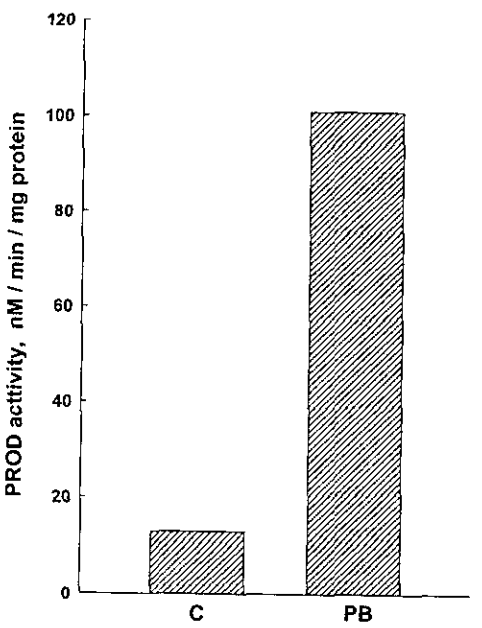

Fig. 3 Effect of phenobarbital on PROD activity of HepG2 cells.

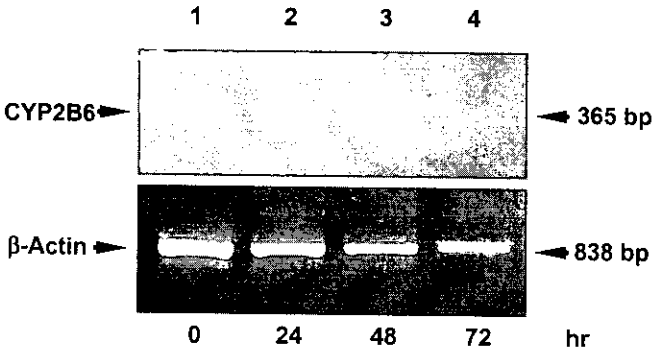

Fig. 4 Effects of phenobarbital on CYP2B6 mRNA of HepG2 cells.

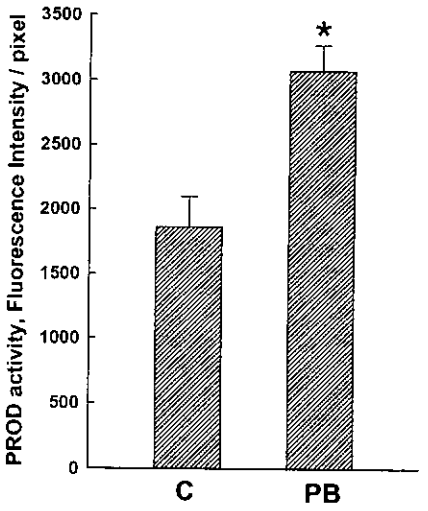

Fig. 6 Quantification of the confocal analysis for phenobarbital-caused an increase in PROD activity in HepG2 cells.

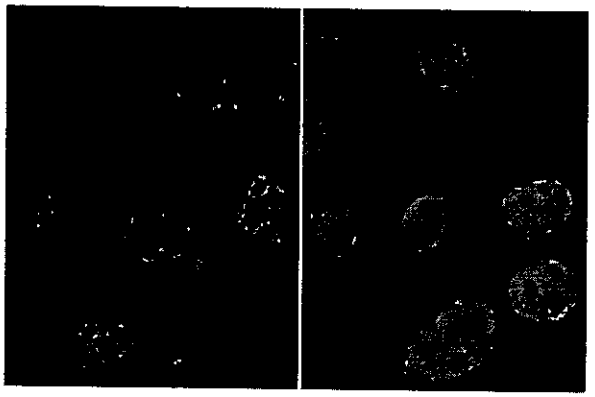

Fig. 5 Confocal analysis of PROD activity in HepG2 cells.